



**HAL**  
open science

## **Pseudomonas produce various metabolites displaying herbicide activity against broomrape**

Tristan Lurthy, Florence Gerin, Marjolaine Rey, Pierre-Edouard Mercier, Gilles Comte, Florence Wisniewski-Dyé, Claire Prigent-Combaret

### ► **To cite this version:**

Tristan Lurthy, Florence Gerin, Marjolaine Rey, Pierre-Edouard Mercier, Gilles Comte, et al.. Pseudomonas produce various metabolites displaying herbicide activity against broomrape. *Microbiological Research*, 2025, 290, pp.127933. 10.1016/j.micres.2024.127933 . hal-04800017

**HAL Id: hal-04800017**

**<https://hal.science/hal-04800017v1>**

Submitted on 23 Nov 2024

**HAL** is a multi-disciplinary open access archive for the deposit and dissemination of scientific research documents, whether they are published or not. The documents may come from teaching and research institutions in France or abroad, or from public or private research centers.

L'archive ouverte pluridisciplinaire **HAL**, est destinée au dépôt et à la diffusion de documents scientifiques de niveau recherche, publiés ou non, émanant des établissements d'enseignement et de recherche français ou étrangers, des laboratoires publics ou privés.



## *Pseudomonas* produce various metabolites displaying herbicide activity against broomrape

Tristan Lurthy<sup>1,\*</sup>, Florence Gerin, Marjolaine Rey<sup>2</sup>, Pierre-Edouard Mercier<sup>3</sup>, Gilles Comte<sup>4</sup>, Florence Wisniewski-Dyé<sup>5</sup>, Claire Prigent-Combaret<sup>6,\*</sup>

Université de Lyon, Université Lyon1, Laboratoire d'Ecologie Microbienne, CNRS UMR-5557, INRAE UMR-1418, VetAgro Sup, 43 Boulevard du 11 Novembre 1918, Villeurbanne 69622, France

### ARTICLE INFO

#### Keywords:

Broomrape  
Fluorescent *Pseudomonas* rhizobacteria  
Metabolomic  
Germination inhibitor  
Bioherbicide

### ABSTRACT

*Pseudomonads* are well-known for their plant growth-promoting properties and biocontrol capabilities against microbial pathogens. Recently, their potential to protect crops from parasitic plants has garnered attention. This study investigates the potential of different *Pseudomonas* strains to inhibit broomrape growth and to protect host plants against weed infestation. Four *Pseudomonas* strains, two *P. fluorescens* JV391D17 and JV391D10, one *P. chlororaphis* JV395B and one *P. ogarae* F113 were cultivated using various carbon sources, including fructose, pyruvate, fumarate, and malate, to enhance the diversity of potential Orobanche growth inhibition (OGI)-specialized metabolites produced by *Pseudomonas* strains. Both global and targeted metabolomic approaches were utilized to identify specific OGI metabolites. Both carbon sources and *Pseudomonas* genetic diversity significantly influenced the production of OGI metabolites. *P. chlororaphis* JV395B and *P. ogarae* F113 produced unique OGI metabolites belonging to different chemical families, such as hydroxyphenazines and phloroglucinol compounds, respectively. Additionally, metabolomic analyses identified an unannotated potential OGI ion, M375T65. This ion was produced by all *Pseudomonas* strains but was found to be over-accumulated in JV395B, which likely explains its superior OGI activity. Then, greenhouse experiments were performed to evaluate the biocontrol efficacy of selected strains: they showed the efficacy of these strains, particularly JV395B, in reducing broomrape infestation in rapeseed. These findings suggest that certain *Pseudomonas* strains, through their metabolite production, can offer a sustainable biocontrol strategy against parasitic plants. This biocontrol activity can be optimized by environmental factors, such as carbon amendments. Ultimately, this approach presents a promising alternative to chemical herbicides.

### 1. Introduction

Within their environment, plants interact with their microbiota influencing their growth and health (Vandenkoornhuys et al., 2015). Among plant growth-promoting rhizobacteria (PGPR), the genus *Pseudomonas* is widely represented and studied for the positive impacts of its members on plants. These bacteria can produce plant beneficial

metabolites such as siderophores, phytohormones, phenazines, cyclopeptides or even 2,4-diacetylphloroglucinol (DAPG) and can interfere with ethylene production through 1-aminocyclopropane-1-carboxylate (ACC) deaminase (Loper et al., 2012; Mishra and Arora, 2018; Shahid et al., 2018; Vacheron et al., 2016). Depending on the plant genotype, the interaction with *Pseudomonas* may be beneficial or not. For example, *Pseudomonas* siderophores, such as pyoverdines, differentially improve

\* Corresponding authors.

E-mail addresses: [tristan.lurthy@univ-lyon1.fr](mailto:tristan.lurthy@univ-lyon1.fr) (T. Lurthy), [marjolaine.rey@univ-lyon1.fr](mailto:marjolaine.rey@univ-lyon1.fr) (M. Rey), [pierre-edouard.mercier@univ-lyon1.fr](mailto:pierre-edouard.mercier@univ-lyon1.fr) (P.-E. Mercier), [gilles.comtes@univ-lyon1.fr](mailto:gilles.comtes@univ-lyon1.fr) (G. Comte), [florence.wisniewski@univ-lyon1.fr](mailto:florence.wisniewski@univ-lyon1.fr) (F. Wisniewski-Dyé), [claire.prigent-combaret@univ-lyon1.fr](mailto:claire.prigent-combaret@univ-lyon1.fr) (C. Prigent-Combaret).

<sup>1</sup> <https://orcid.org/0000-0001-6886-8226>.

<sup>2</sup> <https://orcid.org/0000-0002-3101-5606>.

<sup>3</sup> <https://orcid.org/0009-0007-1010-1373>.

<sup>4</sup> <https://orcid.org/0000-0003-1191-6455>.

<sup>5</sup> <https://orcid.org/0000-0002-2945-0369>.

<sup>6</sup> <https://orcid.org/0000-0001-8968-0660>.

<https://doi.org/10.1016/j.micres.2024.127933>

Received 12 August 2024; Received in revised form 22 September 2024; Accepted 11 October 2024

Available online 22 October 2024

0944-5013/© 2024 The Authors. Published by Elsevier GmbH. This is an open access article under the CC BY license (<http://creativecommons.org/licenses/by/4.0/>).

iron content in graminaceous and dicotyledonous plants (Lurthy et al., 2020; Shirley et al., 2011). Plant tolerance and response to DAPG also vary according to plant species (Brazelton et al., 2008; Keel, 1992). In the context of weed management and the subsequent reduction of crop yield losses, it appears crucial to address the specificity of interactions to find *Pseudomonas* metabolites capable of enhancing crop growth while reducing weed expansion. Indeed, quinoline derivatives produced by a rhizospheric strain, *Pseudomonas aeruginosa* H6, have been described as an efficient bioherbicide (Lawrance et al., 2019). The plant pathogen *P. syringae* 3366 produces a phytotoxin effective against some weeds (Gealy et al., 1996). Additionally, hydrogen cyanide, a volatile compound, has been shown to suppress weed seedling growth (Kremer and Souissi, 2001). Various bacterial mechanisms for regulating weeds have been documented (Hallett, 2005; Mustafa et al., 2019). Parasitic plants like broomrapes are particularly interesting targets for *Pseudomonas*-based bioherbicides. The germination stage is critical in the broomrape life cycle, and *Pseudomonas* strains and their metabolites could significantly affect this step (Brazelton et al., 2008; Kawa et al., 2022; Lurthy et al., 2023; Mustafa et al., 2019).

Broomrapes are obligate root holoparasitic plants belonging to the *Orobanchae* and *Phelipanche* genera in the Orobanchaceae family (Bennett and Mathews, 2006; Joel, 2009). They cause significant damage in intensive crop production systems in Europe and more specifically in the Mediterranean region leading to substantial yield and economical losses. Broomrape infection depends on the host plant and can be either i) host-specific as for *Orobanchae cumana* which can parasitize only sunflower or ii) generalist affecting a wide range of hosts as *Phelipanche ramosa* that parasitizes various crops including hemp (*Cannabis sativa*), tomato (*Solanum lycopersicum*), tobacco (*Nicotiana tabacum*), sunflower (*Helianthus annuus*) and oilseed rape (*Brassica napus*) (Cartry et al., 2021; Parker, 2012). One of the most problematic stages in their parasitic life cycle concerns the production of seeds. Indeed, broomrape produces a large quantity of small seeds per plant and their longevity in soil may last for decades. Moreover, seed germination and haustorium formation are specifically induced by allelochemical signals released from host plant roots. The survival of seeds depends on various abiotic factors (pH, humidity) (Rubiales et al., 2003) and biotic factors (host plants, soil and rhizosphere microbiota) (Huet et al., 2020; Kawa et al., 2022; Martinez et al., 2023; Mutuku et al., 2021). Various agricultural strategies attempt to regulate broomrape populations, such as: i) crop rotation, ii) the induction of suicidal germination of the plant parasitic seeds, iii) the use of less susceptible host plant varieties, iv) the use of chemical herbicides; but no effective curative methods are known yet (Cartry et al., 2021). However, biological control solutions are emerging to limit broomrape infestation, including the use of microorganisms (Cartry et al., 2021; Gibot-Leclerc et al., 2022; Lurthy et al., 2023; Masteling et al., 2019). As a matter of fact, some microorganisms reduce broomrape germination *in vitro* such as *Fusarium oxysporum* (Hasannejad et al., 2006), and *Azo-spirillum brasilense* (Dadon et al., 2004). Recently, the biocontrol activity of phloroglucinol-producing *Pseudomonas* against broomrape was demonstrated using deletion mutants (Lurthy et al., 2023). Although the use of microorganisms is a promising alternative to control parasitic plants, their mode of action and the identification of the metabolites responsible for their inhibitory effect are often still unclear.

In this study, we screened four rhizosphere *Pseudomonas* strains for their ability to inhibit broomrape infection in rapeseed. Two strains have already been characterized genetically and metabolically for their plant-beneficial functions: the reference strain *Pseudomonas ogarae* F113, known to be a good bioherbicide agent against broomrapes (Lurthy et al., 2023) and the *Pseudomonas chlororaphis* JV395B (Rieusset et al., 2020; Vacheron et al., 2016). Two other strains, *Pseudomonas fluorescens* JV391\_D10 and *Pseudomonas fluorescens* JV391\_D17, were selected because they are both taxonomically close but belong to different species than F113 and JV395B. We reported the biological effects of these four strains involved in the Orobanchae-growth inhibition (OGI) in two different experiments, under *in vitro* conditions and in greenhouse. The

OGI activities of the *Pseudomonas* strains were connected to their metabolomic profiles, functional genetic determinants and plant protection activities. We are extending the diversity of metabolites, in addition to DAPG, able to inhibit broomrape at early steps of the life cycle, such as the germination and host root adhesion. All these results aim to highlight the potential of using *Pseudomonas* strains from various species as broomrape biocontrol agents.

## 2. Material and methods

### 2.1. Bacterial strains and media

This study was performed on four strains belonging to three distinct fluorescent *Pseudomonas* subgroups: *Pseudomonas ogarae* F113 which was isolated in 1992 from the rhizosphere of sugar beet (Shanahan et al., 1992), while the three other *Pseudomonas* strains (i.e. *Pseudomonas fluorescens* JV391\_D10 and JV391\_D17, *Pseudomonas chlororaphis* JV395B) were isolated in 2013 from maize rhizosphere soils (Vacheron et al., 2016).

*Pseudomonas* strains were incubated for 72 h at 28 °C, with shaking at 160 rpm, in 10 ml of minimal medium (MM): NH<sub>4</sub>Cl (18.5 mM), KH<sub>2</sub>PO<sub>4</sub> (1 mM), Na<sub>2</sub>HPO<sub>4</sub> (0.8 mM), MgSO<sub>4</sub> (3.25 mM). The MM carbon source solutions were prepared in water, sterilized by filtration on 20-µm filters, and used at 20 mM final concentration for pyruvic acid sodium salt (Sigma-Aldrich, CAS 113-24-6, Saint-Quentin-Fallavier, France), fumaric acid disodium salt (Sigma, CAS 17013-01-3), L-malic acid disodium salt (Sigma, CAS 138-09-0) or fructose (Sigma, CAS 57-48-7). Cultures were centrifuged and supernatants were filtered, adjusted at pH 7 and stored at -20 °C prior to metabolomic analysis and evaluation of their biological effects on broomrape germination.

### 2.2. *Pseudomonas* genomes

Genomic DNA was extracted from overnight cultures of strains JV391\_D10 and JV391\_D17 using a Nucleospin Tissue kit (Macherey Nagel, 740952.50, Hoerdt, France). The DNA was sequenced at Mr. DNA (Shallowater, TX, USA) using MiSeq Illumina technology, generating a 2 × 300 bp paired-end library. Sequences were trimmed and *de novo* assembled with NGen V14 (DNASTar) using default settings, with assembly parameters based on the average size of *P. fluorescens* genomes. Genome analyses were conducted using the MicroScope web platform. Draft genomes of the *Pseudomonas* strains have been deposited in NCBI under BioProject ID PRJNA565121, sample SAMN12734735, with genome accession GCA\_008630545.1 for *Pseudomonas chlororaphis* JV395B, BioProject ID PRJNA572594, sample SAMN12796400, with run accession SRR10166148 for *Pseudomonas fluorescens* JV391\_D10, and BioProject PRJNA572595, sample SAMN12796437, with run accession SRR10166144 for *Pseudomonas fluorescens* JV391\_D17. The accession number for the *P. ogarae* F113 genome is CP003150.1.

A taxonomic tree was inferred through multilocus sequence analysis (MLSA) using four markers: *gyrB*, *rpoB*, *rpoD*, and *rrs*. Distance-based phylogenetic trees were generated using the Neighbor-Joining (NJ) algorithm. Tree topology was assessed with 1000 bootstrap replicates using MEGA-X (Version 10.2.2).

### 2.3. Plant material

Seeds of *Phelipanche ramosa* were collected in France as described by Huet et al. (2020) from broomrape-parasitized plants of winter oilseed rape (*Phelipanche ramosa* pv. oilseed rape) and tobacco (*Phelipanche ramosa* pv. tobacco). Seeds of *Orobanchae cumana* pv. sunflower were provided by Terres Inovia in 2016. All seeds were dry-stored in the dark at 4 °C until use.

Seeds of *Brassica napus*, cultivar AMAZZONITE, were provided by the breeder company RAGT 2n (France) and were dry-stored in the dark at room temperature until use.

#### 2.4. Broomrape seed conditioning and evaluation under in vitro conditions of OGI activity of *Pseudomonas supernatants* and of chemical standards

Broomrape seeds were surface-disinfected and conditioned according to Lurthy et al. (2023). Fifteen microliters of the seed solution were distributed into 96-well plates (Cellstar; Greiner Bio-One, France), with approximately 30 seeds per well. The synthetic strigolactone analogue GR24 (Chiralix, Nijmegen, NL) was used to induce broomrape seed germination. GR24 was resuspended in acetone and then diluted to 10  $\mu\text{M}$  in a 1 mM sodium-potassium phosphate buffer, pH 7.5. Ten microliters of the 10  $\mu\text{M}$  GR24 solution were added to each well. Seventy-five microliters of bacterial supernatants (4-fold diluted) or chemical standard solutions were then added to each well to achieve a final volume of 100  $\mu\text{l}$ . Negative controls were prepared using 75  $\mu\text{l}$  of fresh MM medium (also 4-fold diluted) supplemented with the appropriate carbon source at 20 mM, according to the tested supernatants or 75  $\mu\text{l}$  of phosphate buffer with proper solvent for chemical standard. After 10 days of incubation at 21 °C in the dark, the percentage of germinated broomrape seeds was counted under a binocular microscope (Leica) using Zen 2.3 software. Each experiment with pure molecules and bacterial supernatants was performed independently, 4 and 6 times, respectively.

#### 2.5. Pot experiments

*Brassica napus* cultivar AMAZZONITE seeds were surface-disinfected by soaking for 5 min in a sodium hypochlorite solution with 9.6 % active chlorine, followed by five rinses with sterile water. The seeds were then pre-germinated for 24 h in the dark at 21 °C on water-soaked Whatman paper in a Petri dish. After pre-germination, the seeds were sown in 2 L pots containing broomrape seeds (1 rapeseed seed per pot), as described by Lurthy et al. (2023). Two types of controls were established: one with *P. ramosa* pv. oilseed rape seeds and one without, both without bacterial treatments. For each condition, 18 pots (or 10 pots for the control without broomrapes) were prepared. The soil mixture used was composed of one-third natural loamy soil collected from the experimental farm in La Côte-St-André (France; 16.2 % clay, 43.9 % silt, and 39.9 % sand, pH 7.0 in water; 2.1 % organic matter), one-third vermiculite, and one-third TS3 peat-based substrate (Klasmann-Deilmann GmbH, Geeste, Germany). Soil humidity was maintained at 70 % of field capacity. Each pot was filled with 1 l of free-broomrape soil mixture and then further filled with another liter of soil mixture contaminated with non-disinfected seeds of *Phelipanche ramosa* pv. oilseed rape leading to a final density of 3.9 mg of seeds per pot corresponding to approximately 300 seeds per liter of soil. The experiment was conducted under controlled conditions with a 16-hour light and 8-h dark photoperiod at 25 °C and 50–70 % relative humidity in a greenhouse for 50 days.

At 30 days, 100 ml of NPK amendments (PlantProd 15-15-30: 15 % nitrogen, 15 % phosphate, and 30 % potassium) were applied once a week at a concentration of 1 g/L to support the growth of oilseed rape plants. For inoculation, different *Pseudomonas* strains were cultured for 24 hours at 28 °C in a modified AB medium composed of AB salts [MgSO<sub>4</sub> (1.2 mM), CaCl<sub>2</sub> (70  $\mu\text{M}$ ), NH<sub>4</sub>Cl (18 mM), KCl (2 mM), FeSO<sub>4</sub> (9  $\mu\text{M}$ )], AB phosphate buffer diluted tenfold [K<sub>2</sub>HPO<sub>4</sub> (1.725 mM) and NaH<sub>2</sub>PO<sub>4</sub> (960  $\mu\text{M}$ )], and pyruvate (20 mM) as the carbon source. Bacterial cultures were adjusted to a concentration of  $2 \times 10^6$  CFU/ml, and the appropriate volume was transferred and topped up with filtered supernatant (5 ml  $\times$  18 pots per condition = 90 ml of filtered supernatant). Five milliliters of these bacterial suspensions were sprayed at the base of the plant stem. For negative controls, 5 ml of AB medium with 20 mM pyruvate was applied as a non-inoculated control. Treatments were applied twice during the experiment: first when *B. napus* had 2–4 leaves, and second at 6–8 leaves.

After 50 days, the root systems were sampled, and the adhering soil

was thoroughly removed by hand. Broomrapes attached to each root system were collected, classified by developmental stage (using the infectivity scale in Fig. S4), and counted. The shoot and root dry biomasses of *B. napus* were also measured after drying for 3 days at 70 °C in an oven.

#### 2.6. Metabolomic analyses of *Pseudomonas supernatants*

Identification of metabolites was conducted on 1.5 ml of bacterial culture supernatants for each condition. First, supernatants were lyophilized using a Martin Christ Alpha 1–4 LSC (Osterode, Germany) prior to solid/liquid extraction with methanol. Samples were sonicated for 20 min, then centrifuged for 20 min at 15,000 g, and the supernatants were recovered. The extraction protocol was repeated, yielding a total extracted volume of 3 ml per sample. The organic phase (methanol) was dried using a SpeedVac (Centrivap Cold Trap Concentrator; LABCONCO Co., MO, USA). Dried extracts were resuspended in 100  $\mu\text{l}$  of methanol and centrifuged for 10 min at 5000 g to pellet the remaining solid phase.

One hundred microliters of the supernatant were then transferred into vials and processed for ultra-high pressure liquid chromatography coupled with UV and mass spectrometry (UHPLC-UV-MS) analysis, as previously described by Rieusset et al. (2020). A quality control (QC) sample was prepared by mixing 2  $\mu\text{l}$  of each of the 60 samples to monitor analytical repeatability during UHPLC-MS analysis.

The molecules used as standards in the metabolomic analyses are listed in Table S1. Secondary metabolites were analyzed according to Rieusset et al. (2020), and chromatograms were processed using MassHunter Qualitative Analysis B.07.00 software (Agilent Technologies). Ion identification was performed using chemical standards and the MetaboAnalyst 6.0 database (Pang et al., 2024).

#### 2.7. Identification of OGI molecules in *JV395B* by bio-guided fractionation

Bioguided fractionation was performed on the culture supernatant of *JV395B* grown in fructose. Minimal medium with 20 mM fructose was selected due to the presence of inhibitors in the supernatant. The dried supernatant extract was dissolved in water at a concentration of 80 mg/ml and subjected to preparative HPLC in 15 injections of 100  $\mu\text{l}$  each (using an Agilent Eclipse XDB-C18 (9.4  $\times$  250 mm, 5 micron) column). HPLC analyses were conducted at a flow rate of 3.4 ml/min at 40 °C, using a solvent gradient with solvent A (water with 0.4 % formic acid, v/v) and solvent B (acetonitrile). After an initial 3 min at 2 % solvent B, the proportion of solvent B was increased to 36 % over 11 min (Fractions 1–11), then from 36 % to 100 % over 6 min (Fractions 12–18), followed by a 5-min isocratic phase with 100 % solvent B (Fractions 19–23). A total of 23 fractions were collected between 2 min and 25 min (1 min per fraction). Fractions corresponding to each elution range from each run were pooled and dried using a SpeedVac or lyophilization. After fractionation, each fraction was tested for its activity on broomrape germination.

#### 2.8. Data processing, statistical analysis and metabolite identification

Data were analyzed using R Studio (v.4.2.1) and considered significantly different when the p-value was < 0.05. The data were assessed for normal distribution and variance homogeneity using Shapiro-Wilk and Bartlett tests, respectively. When these assumptions were met, ANOVA was performed, followed by an LSD-Fisher test. If the assumptions were not met, Kruskal-Wallis tests were used to detect differences between conditions.

Metabolomic analysis was conducted using the collaborative Galaxy platform 'Workflow4metabolomics' (Giacomoni et al., 2015) with the same parameters as described in Rieusset et al. (2020). Principal component analysis (PCA) and distance matrix analysis using the "bray" method were performed with the R package factoextra. The adonis2

function from the “vegan” package was used for PERMANOVA analyses. The “pheatmap” package was used for heatmap profiling and clustering.

### 3. Results

#### 3.1. Inhibitory activity of *Pseudomonas* supernatants

The production of putative Orobanche-growth inhibitor (OGI) was investigated in four *Pseudomonas* strains belonging to the *P. fluorescens* subgroup (JV391\_D17 and JV391\_D10), the *P. chlororaphis* subgroup (JV395B) and the *P. corrugata* subgroup (F113) (Fig. S1). Different carbon sources were used to grow the strains, in order to increase the diversity of secondary metabolites produced by these 4 strains. Prior to finalizing the choice of carbon source, we conducted preliminary experiments to identify carbon sources that would support robust bacterial growth and distinct supernatant activities. Pyruvic acid, fumaric acid, malic acid, fructose, glucose, glycerol, mannitol, and succinate were included in this pre-screening but the last four were not retained; glucose did not sustain robust bacterial growth, glycerol alone completely inhibited broomrape germination, mannitol exhibited a similar inhibitory activity than that observed with fructose, a carbon source extensively used in previous studies (Lurthy et al., 2023).

Prior to testing supernatant activity on broomrape seeds, the four selected carbon sources were examined as potential OGI molecules on the three selected broomrape pathovars (chosen on the basis of different host specificity). Pyruvate and fructose showed inhibitory effects at concentrations higher than 12.5 mM on all broomrapes while malate and fumarate inhibit the germination rate at concentrations higher than 250 μM on *P. ramosa* pv. sunflower but not on *O. cumana* and *P. ramosa* pv. Tobacco, for which concentrations higher than 2 mM are required to inhibit their germination (Table S2). Besides, the presence of residual

malate in the supernatant was quantified using a malate assay kit (Megazyme, cat. no. K-LMAL-116A). Almost all malate was consumed (residual concentrations were below the detection limit of 200 μM) by the four strains (Table S3). Residual fumarate was also estimated by UHPLC-UV-MS in comparison to a control sample containing 1 mM Fumarate in MM (Fig. S2). All *Pseudomonas* supernatants contained less than 1 mM of residual fumarate. Since bacterial supernatants were diluted four times when applied on broomrape, the residual concentrations of the chosen carbon sources were not considered as giving OGI activities under *in vitro* conditions. Thus, any OGI activity of bacterial supernatants could be linked to the production of potential OGI molecules by the strains.

The OGI activity of bacterial supernatants was then studied on the three broomrape pathovars and appeared to be dependent on broomrape species, carbon sources and tested strains (Table 1). Susceptibility to OGI metabolites differed among broomrapes pathovars. *P. ramosa* pv. tobacco appeared to be less inhibited by bacterial supernatants than *O. cumana* pv. sunflower or *P. ramosa* pv. rapeseed. The most significant OGI effects of *Pseudomonas* supernatants were overall observed on *P. ramosa* pv. rapeseed (Table 1).

The use of different carbon sources made it possible to observe dissimilar OGI effects. Malate induced the least OGI activity, whereas fumarate appeared as the one allowing OGI activity against all broomrapes. Pyruvate and fructose have intermediate effects on OGI production, depending on the broomrape pathover and the tested *Pseudomonas* strain.

Under the tested conditions, JV391\_D17 showed no OGI effect, except with fumarate as carbon source for 2 broomrapes: *P. ramosa* pv. rapeseed, and *O. cumana* pv. sunflower. JV391\_D10 supernatants exhibited OGI effects in the presence of all four carbon sources, but activity levels were dependent on broomrape genotypes. JV395B

**Table 1**  
Germination rate of broomrape in diluted supernatants of bacterial cultures.

Strain	Species	Pyruvate			Fumarate			Malate			Fructose		
		<i>P. ramosa</i> 1 pv. rapeseed	<i>P. ramosa</i> 2 pv. tobacco	<i>O. cumana</i> pv. sunflower	<i>P. ramosa</i> 1 pv. rapeseed	<i>P. ramosa</i> 2 pv. tobacco	<i>O. cumana</i> pv. sunflower	<i>P. ramosa</i> 1 pv. rapeseed	<i>P. ramosa</i> 2 pv. tobacco	<i>O. cumana</i> pv. sunflower	<i>P. ramosa</i> 1 pv. rapeseed	<i>P. ramosa</i> 2 pv. tobacco	<i>O. cumana</i> pv. sunflower
JV391D17	<i>P. fluorescens</i>	95 ± 4 <sup>a</sup>	92 ± 6 <sup>a</sup>	85 ± 3 <sup>a</sup>	39 ± 8 <sup>a</sup>	96 ± 5 <sup>a</sup>	70 ± 6 <sup>a</sup>	79 ± 4 <sup>a</sup>	95 ± 1 <sup>a</sup>	79 ± 3 <sup>a</sup>	89 ± 3 <sup>a</sup>	100 ± 3 <sup>a</sup>	79 ± 7 <sup>a</sup>
JV391D10	<i>P. fluorescens</i>	48 ± 6 <sup>ab</sup>	88 ± 4 <sup>a</sup>	44 ± 4 <sup>b</sup>	11 ± 3 <sup>ab</sup>	68 ± 10 <sup>ab</sup>	37 ± 7 <sup>b</sup>	54 ± 3 <sup>b</sup>	86 ± 3 <sup>a</sup>	52 ± 4 <sup>b</sup>	65 ± 3 <sup>b</sup>	98 ± 9 <sup>a</sup>	55 ± 4 <sup>a</sup>
JV395B	<i>P. chlororaphis</i>	23 ± 4 <sup>b</sup>	8 ± 3 <sup>b</sup>	46 ± 7 <sup>ab</sup>	31 ± 6 <sup>a</sup>	37 ± 12 <sup>b</sup>	49 ± 8 <sup>ab</sup>	84 ± 3 <sup>a</sup>	65 ± 4 <sup>b</sup>	59 ± 6 <sup>a</sup>	19 ± 2 <sup>c</sup>	0 ± 0 <sup>b</sup>	22 ± 3 <sup>b</sup>
F113	<i>P. ogarae</i>	14 ± 9 <sup>b</sup>	86 ± 4 <sup>a</sup>	30 ± 13 <sup>b</sup>	5 ± 2 <sup>b</sup>	69 ± 13 <sup>ab</sup>	34 ± 6 <sup>b</sup>	86 ± 3 <sup>a</sup>	92 ± 3 <sup>a</sup>	93 ± 4 <sup>a</sup>	88 ± 7 <sup>a</sup>	86 ± 8 <sup>a</sup>	76 ± 6 <sup>a</sup>
ANOVA, KW p-value		0.0005393***	3.486e-10 ***	0.009365**	0.004 ***	0.01976 *	0.0139*	2.929e-05***	3.844e-05***	5.078e-05***	2.944e-09 ***	0.002971**	6.646e-06 ***

Supernatants were diluted 4 times. † Percentage of broomrape germination compared to control medium without bacterial supernatant expressed as mean ± standard error (n= 6). The different lowercase letters a,b,c represent statically different groups by column (Anova with post-hoc Fisher’s LSD and correction of Bonferroni, p-value < 0.05 or Kruskal-Wallis with post-hoc Dunn test and correction Bonferroni, p-value < 0.05). Green, yellow and red boxes illustrate > 75 %, between 75 % and 25 % and < 25 % of broomrape germination respectively.

**Table 2**  
General genomic characteristics of the 4 *Pseudomonas* strains.

Characteristics	JV391_D17	JV391_D10	JV395B	F113
Specie group	<i>P. fluorescens</i>	<i>P. fluorescens</i>	<i>P. chlororaphis</i>	<i>P. ogarae</i>
Plant origin	Maize	Maize	Maize	Sugar beet
Genome size (Mpb)	6.92	7.17	6.79	6.85
G + C (%)	60.68	60.54	63.08	60.78
Protein coding sequences	6640	6936	6550	6340
Coding (%)	89.93	89.69	88.06	87.91
tRNA	56	56	60	66
rRNA	8	6	8	16
Coding DNA Sequences (CDS)	6640	6936	6550	6340
Pan CDS	6329	6924	6520	6329
Core CDS (%*)	3085 (46.5 %)	3089 (44.6 %)	3093 (47.4 %)	3086 (48.8 %)
Var CDS (%*)	3544 (53.5 %)	3835 (55.4 %)	3427 (52.7 %)	3243 (51.2 %)
Strain specific CDS (%*)	538(8.1 %)	773 (11.2 %)	2621 (40.2 %)	2381(37.6 %)

\* Percent compared to total CDS.

produced OGI molecules in presence of the four carbon sources, but more abundantly with pyruvate and fructose, regardless of the broomrape genotype. F113 produced effective OGI molecules, with pyruvate and fumarate being the most potent carbon sources for this bioherbicide activity, and with the strongest activity observed on *P. ramosa* pv. rapeseed.

### 3.2. Characteristics of *Pseudomonas* strains: genome mining and metabolomic analyses of their supernatants

To better understand the differences and similarities observed between the four strains in their OGI production, we first looked at their genome. *Pseudomonas* strains JV391\_D17, JV391\_D10, JV395B and F113 have genome sizes of 6.92, 7.17, 6.79 and 6.85 Mbp, respectively (Table 2). Their GC percentages are quite similar, around 60 %, with the exception of JV395B which is at 63 %. The percentage of strain-specific CDS is lower in JV391\_D17 (8.1 %) and JV391\_D10 (11.1 %) than in JV395B (39.9 %) and in F113 (37.2 %) because the strains JV391\_D17 and JV391\_D10 share a large number of genes, corresponding to 92 % and 89 % of their total genomes, respectively.

The four genomes were explored for their functional plant-beneficial traits (see Table S4). All four genomes contain genes associated with the synthesis of pyoverdine (*pvd* genes), indole-3-acetic acid (*iaaM*), nitric oxide (*nirK/S*), and pyrroloquinoline quinone (*pqqC*). However, the JV395B genome uniquely includes genes responsible for the biosynthesis of pyrrolnitrin and phenazine. Additionally, the F113 strain is the only one capable of producing DAPG and its derivatives.

Among the two strains in the *P. fluorescens* subgroup, JV391\_D17 and JV391\_D10, their functions are largely similar, except that JV391\_D17 alone contains the ACC deaminase gene (*acdS*). Compared to JV395B and F113, these two strains also possess the *acoRABC* genes, which are involved in the biosynthesis and catabolism of acetoin.

Overall, the genome mining revealed that JV391\_D10 and JV391\_D17 lack gene clusters for the biosynthesis of secondary metabolites with potential antagonistic activity against prokaryotic or eukaryotic cells, unlike those in JV395B and F113. No gene encoding the biosynthetic pathways for pyoluteorin was found in any of the four genomes (see Table S4).

Taking into account differences in OGI effects, we undertook to analyse the molecular composition of supernatants. To that end, a MeOH extraction was performed and samples were analyzed by UHPLC-UV-MS (UV; MS in negative and positive ionization mode). Data processing (setting parameters in Table S5) resulted in the construction of two data matrices containing 548 and 516 peaks for positive and negative ionization modes, respectively. The retention times and intensities of signals were reproducible and stable throughout the analytical process, indicating the reliability of the metabolomic investigation. Data matrixes obtained from chromatographic profiles were further compared by principal component analysis (PCA).

In the positive ionization mode, biological replicates from the same modality cluster on the principal component analysis, revealing good reproducibility. PCA of all supernatants showed a principal discrimination between strains (Fig. 1A). Except for the fructose condition, the supernatant compositions of F113 and JV395B were generally separated from those of JV391\_D17 and JV391\_D10 on PC2 (12.7 %). In addition, the composition of fructose supernatants appeared less different between strains and, except for JV395B, fructose supernatants were strongly separated from those of other carbon sources along PC1. JV395B supernatants from all carbon sources were closer to each other than for all other strains. Principal component analyses performed for strains according to carbon sources showed that ion composition obtained with simple sugar, such as fructose, was different from those obtained with organic acids and separated along PC2 (Fig. 1B). Regarding ions produced in presence of each carbon source according to *Pseudomonas* strains, JV391\_D17 and JV391\_D10 shared similar composition, whereas those of JV395B and F113 differed from each

other (separated by PC1 and PC2) (Fig. 1C).

In the negative ionization mode, the clustering was more heterogeneous than in the positive mode, especially for F113 supernatants and pyruvate supernatants, for which there was no clear discrimination (Fig. S3ABC).

Then, positive ion matrices were explored in JV395B and F113, in order to identify the discriminant compounds likely involved in OGI activity. Heatmaps associated with clustering of the closest ions allowed us to visualize the distribution of discriminating metabolites according to their accumulation in the different media (Fig. 2A, Fig. S4A).

Regarding F113, the identification of discriminant compounds linked to the highest OGI was possible for supernatants obtained in the presence of pyruvate and fumarate. The ions M169T226 and M170T226, associated with mono-acetylphloroglucinol (MAPG), and the ion M212T390, linked to 2,4-diacetylphloroglucinol (DAPG), were thus identified as broomrape inhibitors, confirming our previous results (Lurthy et al., 2023) (Fig. S4).

However, none of the metabolites associated with JV395B are known to inhibit plant growth. To investigate further, ions from the different supernatants of *Pseudomonas* JV395B were analyzed. Specifically, we focused on ions that accumulated more in supernatants with fructose and pyruvate as carbon sources (Cluster 8, Fig. 2A). Despite substantial annotation efforts and comparisons of spectral data with literature and UPLC-UV-MS analyses of chemical standards, none of the discriminant compounds in cluster 8 could be annotated.

Thus, we conducted a fractionation of the JV395B fructose supernatant. OGI activity was identified in fraction 1, corresponding to highly polar ions detected by the mass chromatograph during the first 90 s (Fig. 2B). By focusing on these highly polar ions, we correlated the accumulation of Cluster 8 ions with OGI activities against the three broomrapes. Several ions, showing the strongest negative correlation (indicating better OGI activity as the quantity of the molecule increases in the supernatant), were examined for their accumulation in the supernatants of the other three strains (Fig. 2C). Only the ion M375T65 correlated with the OGI activity observed in all four *Pseudomonas* supernatants (Table 1). Online databases of Metaboanalyst suggested that M375T65 as being “isocucurbit acid glucoside”, but its real identity requires further analysis (Fig. 2D).

### 3.3. Identification of new secondary metabolites of *Pseudomonas* strains with bioherbicide activities based on comparative metabolomics and genomics

In parallel with the exploratory metabolomic analyses, we employed a targeted approach to identify the OGI activity of commercially available *Pseudomonas* molecules. These molecules were either i) present in the studied supernatants or ii) identified in the literature as having inhibitory effects on plants, such as indole-3-acetic acid, salicylic acid, cytokinin, and pyoluteorin (García de Salamone et al., 2001; Mishra and Arora, 2018; Sosnowski et al., 2023; Spaepen et al., 2014) or as belonging to the same biosynthesis pathway of herbicide (Cain et al., 2003). Additionally, we examined the accumulation of dicarboxylic or tricarboxylic acids (malate, succinate, fumarate, and citrate) in *Pseudomonas* media, which had been previously studied for their OGI activity on *Striga*, another parasitic plant (Bally et al., 2017).

Salicylic acid was detected in all *Pseudomonas* supernatants (Table 3). Di- and tricarboxylic acids as malate and citrate were more widely detected in JV391\_D17 and JV391\_D10 supernatants whereas succinate and fumarate were more often detected in JV395B and F113 supernatants. Dimethyl 2,6-pyridinedicarboxylate, DAPG and its derivatives such as PG and MAPG were detected specifically in F113 supernatants. DAPG and its derivatives were produced in higher quantity with pyruvate and fumarate as carbon sources (LC-UV detection, Table S6). Phenazines (PCA and OH-PHZ) were detected only in JV395B supernatants, and when grown in presence of the four carbon sources. OH-PHZ was produced at levels below the OGI threshold with

supernatants of cultures grown in pyruvate, malate, and fumarate, and it was undetectable with the fructose supernatant (Table S7). Indole-3-acetic acid (IAA), trans-zeatin, pyrrolnitrin and pyoluteorin were not detectable with our analytical method (Table 3).

For each available standard molecule, we determined the minimum inhibitory concentration required to inhibit at least 50 % of broomrape seed germination. Pure molecules were tested only on *P. ramosa* pv. rapeseed and *O. cumana* pv. sunflower because, the presence of 0.33 %

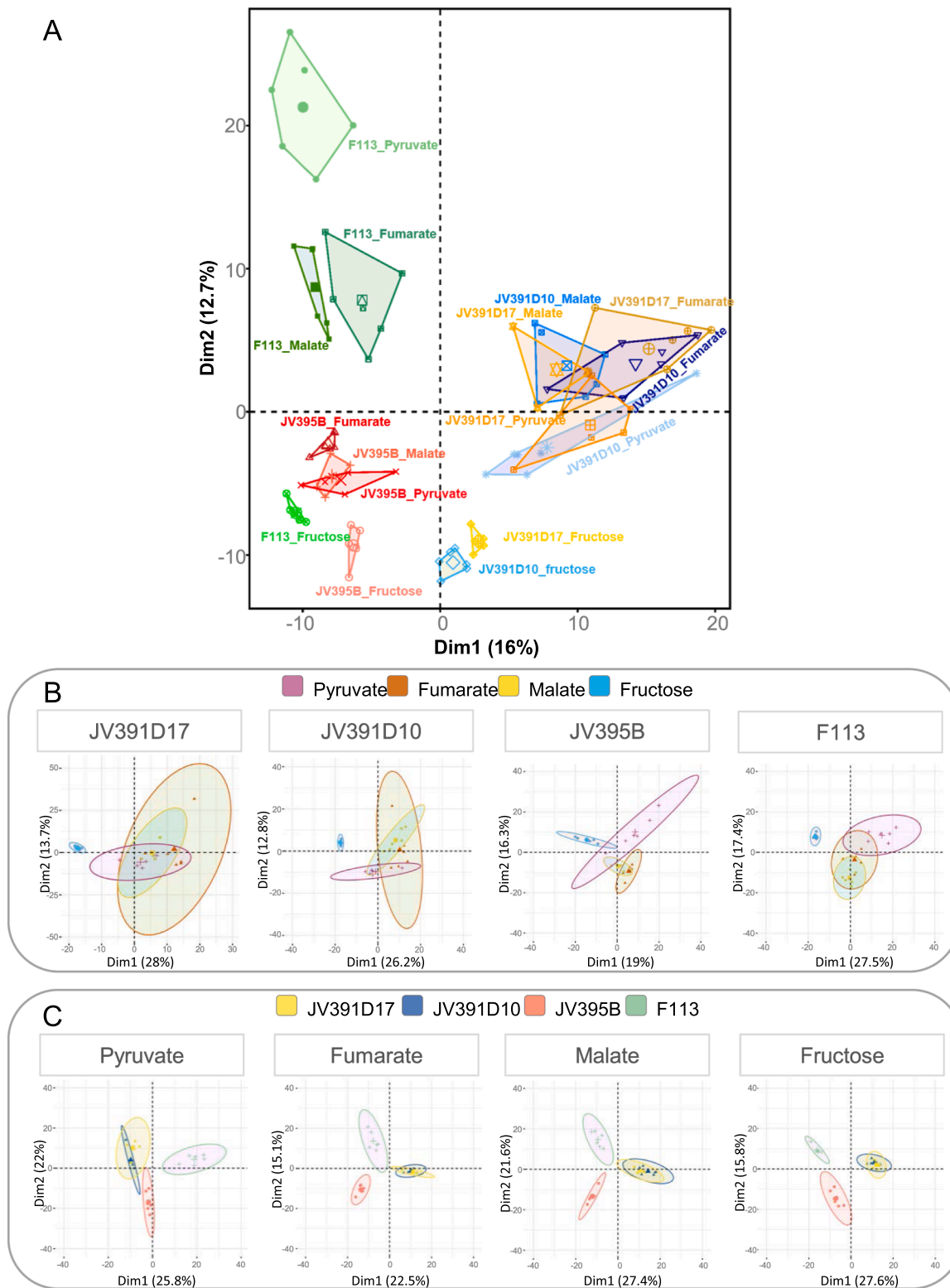
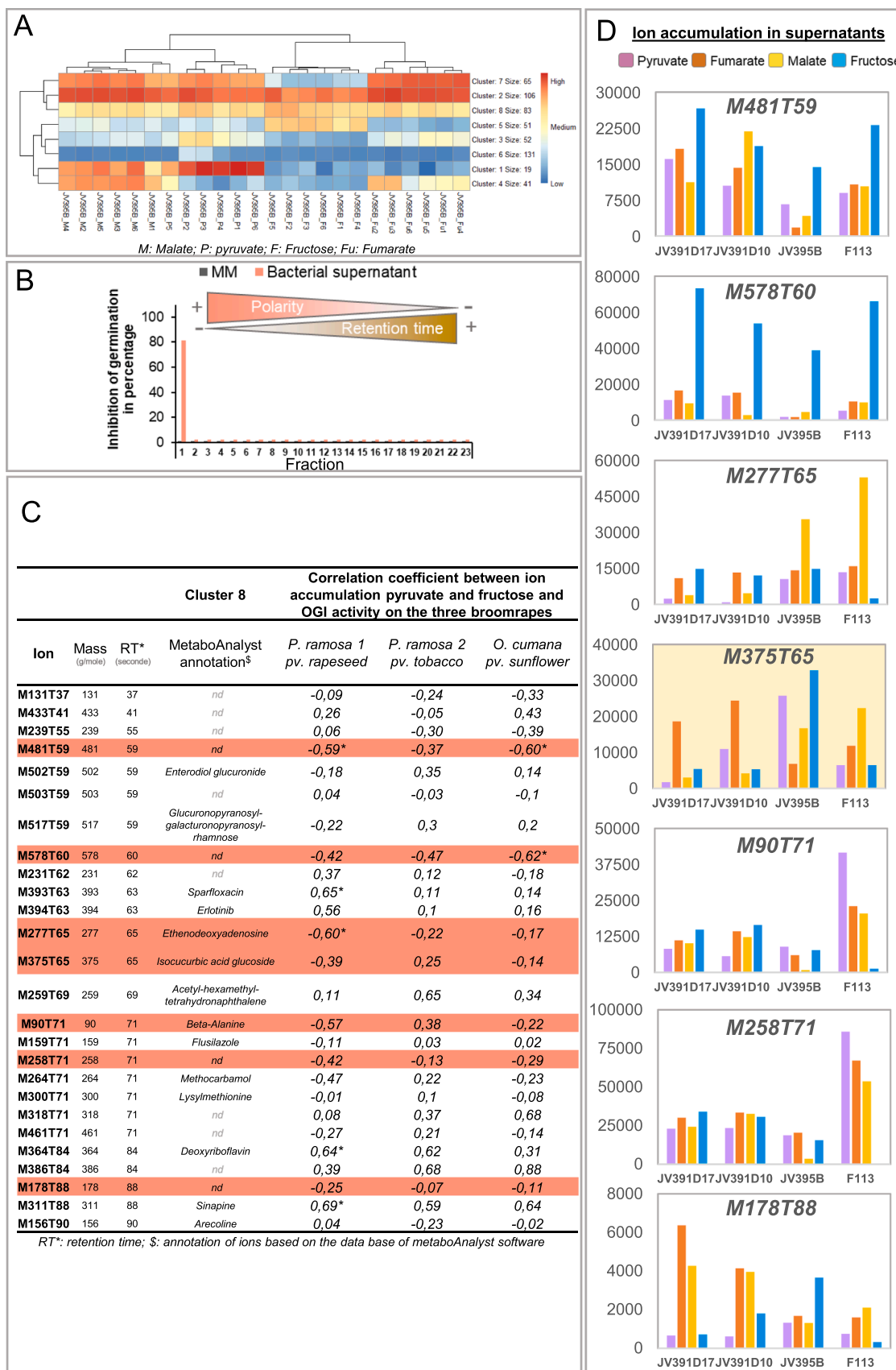


**Fig. 1. Impact of strains and carbon sources on *Pseudomonas* metabolomes.** Principal component analyses of the ion composition of *Pseudomonas* supernatants were obtained from UHPLC-MS profiles of supernatants from each of four *Pseudomonas* strains grown in the presence of different carbon sources, in positive mode ionization (n = 24 samples; 548 ions). **A:** PCA of ions contained in the total supernatants. **B:** PCA of ions produced by strains according to carbon sources. **C:** PCA of ions produced in each carbon source according to strains. In **B** and **C**, ellipses indicate the 0.95 confidence level.



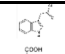
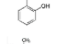
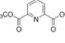
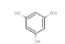
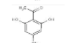
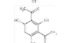
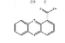
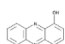
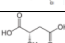
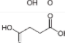
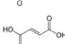
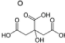
(caption on next page)



**Fig. 2. Identification of potential OGI ion candidates in supernatant of *Pseudomonas* JV395B in positive mode.** A: Heatmap profiling associated to ion accumulation in JV395B supernatants. Ions were clustered according to accumulation patterns. B: Culture supernatant fractionation of JV395B in fructose medium by bioguided fractionation. After the fractionation, each fraction was tested to evaluate its activity on broomrape germination. C: Correlation between OGI activity observed against the three broomrapes and ions present in cluster 8 associated, with the group of ions more abundantly produced in both fructose and pyruvate medium than in fumarate and malate medium. Only ions with a retention time of less than 90 s, corresponding to polar molecules potentially contained in fraction 1, were investigated. Colored ions are representing candidate ions with negative correlation coefficient corresponding to decreased Orobanche germination rate as their quantity increases in the supernatant. D: Accumulation of candidate ions in the different media and in the different *Pseudomonas*. Their accumulation is represented by the arbitrary intensity detected by mass spectrometry. The yellow-highlighted ion graph corresponds to the only one polar ion for which a correlation is observed between its accumulation in the four *Pseudomonas* supernatants and the OGI activity of the corresponding supernatants shown in Table 1.

**Table 3**

Chemical characterization and production of metabolites with antagonistic activities against broomrape germination. Detailed chemical characterization and identification of the compounds are presented in Table S5.

Pure molecule activities under <i>in vitro</i> condition		Detected in supernatant by UHPLC-QTOF according to standard								Chemical characteristics							
Compounds Formula	Structure	MIC <sub>50</sub> on <i>P. ramosa</i> pv rapeseed	MIC <sub>50</sub> on <i>O. cumana</i> pv sunflower	JV391D17 <i>P. fluorescens</i>		JV391D10 <i>P. fluorescens</i>		JV395B <i>P. chlororaphis</i>		F113 <i>P. agarum</i>		Mass (g/mol)	[M-H] <sup>+</sup> (m/z)	[M+H] <sup>+</sup> (m/z)	UVλ (nm)	RT (sec)	Ref
				τ	η	ξ	ζ	τ	η	ξ	ζ						
<b>Indole-3-acetic acid</b> C <sub>10</sub> H <sub>9</sub> NO <sub>2</sub>		>50 μM <sup>§</sup>	>50 μM <sup>§</sup>									175.19	174.0562	176.0701	268; 278; 286	257	(Spaepen et al., 2014)
<b>Salicylic acid</b> C <sub>7</sub> H <sub>6</sub> O <sub>3</sub>		>50 μM	>50 μM									138.12	137.0249	nd	302; 236	270	(Li et al., 2022)
<b>Trans-zeatin (cytokinin)</b> C <sub>10</sub> H <sub>13</sub> N <sub>5</sub> O		4 μM	6 μM									219.25	218.1045	220.1215	272	63	(Sosenowski et al., 2023)
Dimethyl 2,6-pyridinedicarboxylate C <sub>8</sub> H <sub>8</sub> NO <sub>4</sub>		> 50 μM	> 50 μM									195.06	nd	196.0609	nd	214	nd
Phloroglucinol C <sub>6</sub> H <sub>6</sub> O <sub>3</sub>		23 μM	79 μM									126.11	125.0243	127.0386	230; 268; 363	57	(Lurthy et al., 2023)
Monoacetylphloroglucinol C <sub>8</sub> H <sub>8</sub> O <sub>4</sub>		43 μM	146 μM									168.1	167.0361	169.0493	228; 286; 333	226	(Lurthy et al., 2023)
2,4-diacetylphloroglucinol C <sub>10</sub> H <sub>10</sub> O <sub>5</sub>		20 μM	29 μM									210.18	209.0474	211.0604	220;270; 328	390	(Lurthy et al., 2023)
Phenazine-1-carboxylic acid C <sub>12</sub> H <sub>8</sub> N <sub>2</sub> O <sub>2</sub>		>50 μM	>50 μM									224.07	nd	225.0688	248; 368; 415	354	nd
Hydroxyphenazine C <sub>12</sub> H <sub>8</sub> N <sub>2</sub> O		33 μM	35 μM									196.07	nd	197.0700	230; 255; 364; 421	282	nd
Pyrrrolnitrin C <sub>10</sub> H <sub>6</sub> Cl <sub>2</sub> N <sub>2</sub> O <sub>2</sub>		30 μM	>50 μM									255.98	254.9729	256.9883	193; 211; 246	438	(Cain et al., 2003)
<b>Pvoluteorin</b> C <sub>11</sub> H <sub>7</sub> Cl <sub>2</sub> NO <sub>3</sub>		0.7 μM	3 μM									270.98	269.9730	271.9876	245 ; 310	330	(Maurhofer et al., 1995)
Malate C <sub>4</sub> H <sub>6</sub> O <sub>5</sub>		416 μM	> 2mM									134.08	133.0130	nd	226	43	(Bally et al., 2017)
Succinate C <sub>4</sub> H <sub>4</sub> O <sub>4</sub>		440 μM	> 2 mM									118.09	117.0175	nd	nd	55	(Bally et al., 2017)
Fumarate C <sub>4</sub> H <sub>4</sub> O <sub>4</sub>		545 μM	> 2 mM									116.07	115.0035	nd	nd	55	(Bally et al., 2017)
Citrate C <sub>6</sub> H <sub>8</sub> O <sub>7</sub>		435 μM	710 μM									192.12	191.0170	193.0346	226	54	(Bally et al., 2017)

\*\* , available commercial molecules were tested at different concentrations (2, 1, 0.5, 0.25, 0.125, 0.0625 mM for organic acids and amino acids or 50, 25, 12.5, 6.25, 3.125 μM for bacterial molecules or hormones). For each molecule, the MIC<sub>50</sub> (Minimum inhibitory concentration 50 %) was estimated according to a logarithmic trend curve obtained on the mean of each concentration tested for *P. ramosa* pv. rapeseed germination inhibition. P, pyruvate; F, fumarate; M, malate; Fr, fructose; [M + H]<sup>+</sup>: positive mode [M-H]<sup>+</sup>: negative mode; ξ, maximum UV-spectral absorbance wavelengths; RT, retention time; Ref, bibliographical references where broomrape germination inhibition activities or negative effects on root or shoot plant growth were demonstrated. Underlined bold compounds correspond to those with inhibitory effects on plants found in the literature. §, not tested at higher concentration because superior to the estimated biological production. White cells: not detected; colored cells: detected in at least 4 out of the 6 tested supernatants (Li et al., 2022; Maurhofer et al., 1995).

<sup>a</sup> \*\* should be added in the first table cell with the word "Compounds"

methanol as a solvent inhibited seed germination of *P. ramosa* pv. tobacco (data not shown). As with supernatants, *O. cumana* was less inhibited by pure molecules than *P. ramosa*. Regarding *P. ramosa*, organic acids were weak inhibitors (MIC<sub>50</sub> = ~400 μM), with a greater activity for malate and citrate. The dimethyl 2,6-pyridinedicarboxylate (specifically produced by F113), the phenazine-1-carboxylic acid (PCA, specifically produced by JV395B) and the hormones such as IAA and salicylic acid did not affect the broomrape germination rate in the tested concentration. Phloroglucinol compounds inhibited both broomrapes and had MIC<sub>50</sub> values ranging from 20 μM for DAPG to 43 μM for MAPG on *P. ramosa*. Pyrrolnitrin and hydroxyphenazine (produced by JV395B) had a similar activity with a MIC<sub>50</sub> of 30 μM. The best inhibitory effect was obtained with pvoluteorin with a MIC<sub>50</sub> at 0.7 μM and 3 μM on *O. cumana* and *P. ramosa* respectively (Table 3).

Thus, some *Pseudomonas* secondary metabolites showed high OGI activity, while others did not.

#### 3.4. Biocontrol activity against *P. ramosa* pv. rapeseed in greenhouse

Given the results of the *in vitro* experiments, *Pseudomonas* JV391\_D10, JV395B and F113 were selected for testing their efficacy as biocontrol agents against *P. ramosa* pv. rapeseed on rapeseed in a greenhouse experiment (Fig. 3), while the less efficient strain JV391\_D17 was put aside. The *Pseudomonas* strains were grown and inoculated with MM pyruvate 20 mM, the most appropriate carbon source due to its low toxicity to broomrape and its ability to induce the production of OGI molecules.

First, the microbial treatments did not impact the shoot biomass of

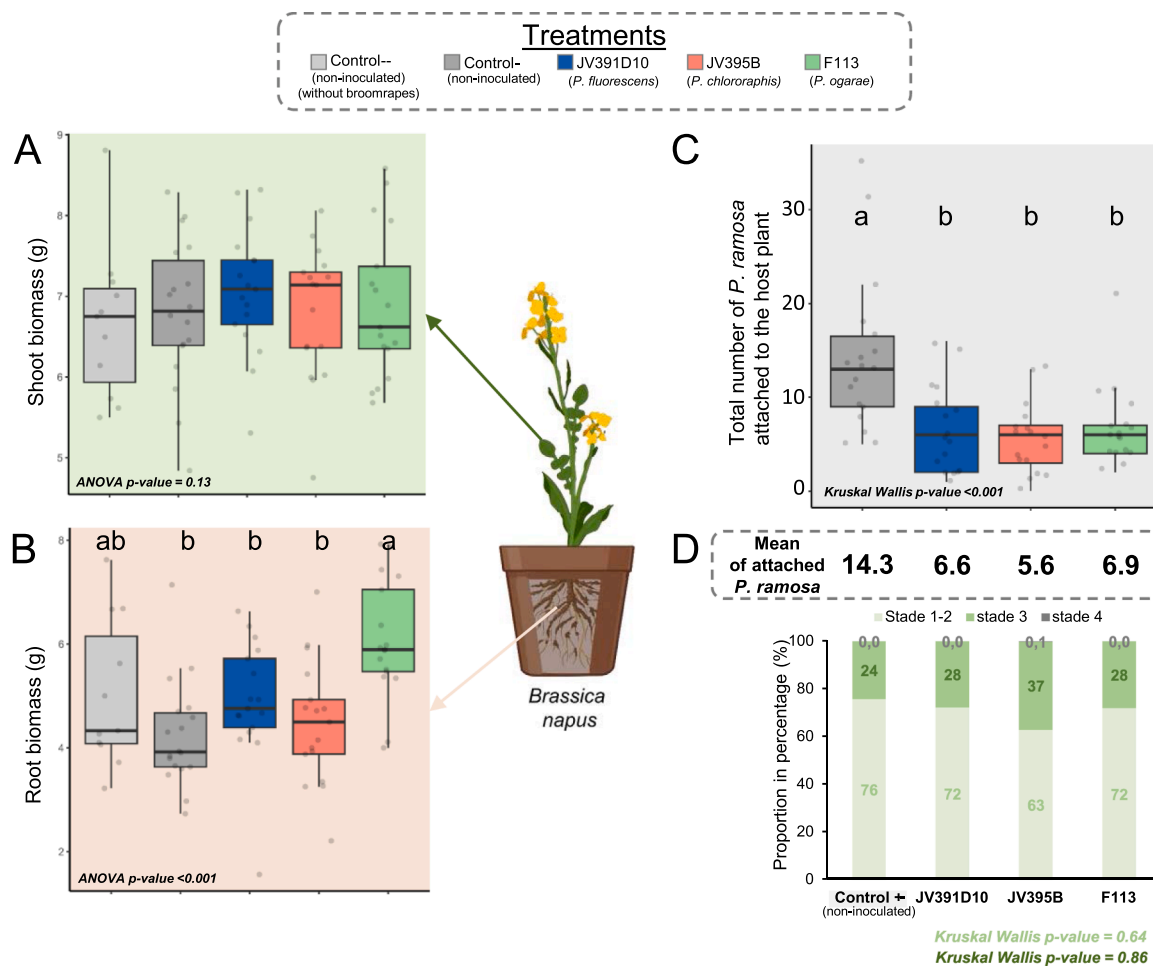


**Fig. 3.** Effect of the inoculation of *Pseudomonas* sp. on the shoot (A) and root (B) biomasses of rapeseed and on broomrape infestation levels (C, D). Different treatments were applied as follows: bacterial inoculants (JV391D10, JV395B, and F113, approximately five milliliters per pot of solutions at  $2 \times 10^6$  bacteria/ml) and two control conditions, which correspond to the application of 5 ml of 10 mM MgSO<sub>4</sub>. The experiment was performed in a mixture containing natural soil artificially infested with approximately 300 *P. ramosa* seeds per liter of soil. Measurements were taken on *Brassica napus* 50 days after sowing. (A) The green background of the boxplots corresponds to rapeseed shoot biomass data, while (B) the brown background is associated with rapeseed root biomass data. (C) Evaluation of the number of attached *P. ramosa* on the root system of *Brassica napus* in a greenhouse. The horizontal lines indicate the interquartile range, with the center representing the median. (D) Proportion of broomrapes attached to the root of *B. napus* according to their developmental stage. The developmental stage of *P. ramosa* was estimated according to the developmental scale available in Fig. S4. Statistical differences were assessed by ANOVA and Kruskal-Wallis test using a Bonferroni correction and are indicated with letters according to post-hoc tests such as Fisher's LSD or Dunn's test, respectively.

rapeseed (Fig. 3A) whereas F113 inoculation improved root biomass compared to the other strains and the non-inoculated controls. Second, treatments with *Pseudomonas* negatively impacted *P. ramosa* infestation. Indeed, compared to the negative control inoculated with broomrape alone, the number of broomrapes attached on rapeseed roots was approximately 50 %, 55 % and 60 % lower for samples inoculated with F113, JV391\_D10 and JV395B, respectively (Fig. 3C). Microbial treatments did not affect the proportion of broomrapes at the different developmental stages (Fig. 3D).

#### 4. Discussion

Plant growth-promoting bacteria such as pseudomonads are well characterized for their protective effect on crops against plant pathogens (Lee et al., 2022; Müller and Behrendt, 2021). Their biocontrol capacity against microbial phytopathogens has been shown to be related to the production of specific antimicrobial compounds. In this study, pseudomonad biocontrol activity was evaluated for extension to crop protection against parasitic plants, which is a growing problem in the field

nowaday.

##### 4.1. OGI metabolite production in *Pseudomonas* is influenced by both carbon sources and strain genetic diversity

To investigate the production of OGI metabolites, four *Pseudomonas* strains were grown in the presence of different carbon sources: a simple sugar (fructose) or di- and tri-carboxylic acids directly involved in the Krebs cycle (pyruvate, fumarate and malate). While fumarate is transformed into malate in the Krebs cycle, pyruvate is a precursor of acetyl-coenzyme A, which is integrated into the cycle by combining with oxaloacetate. These carbon sources resulted in varying OGI activities and metabolomes among the strains. The metabolomes were less variable and distinct with fructose compared to those obtained with organic acids, with organic acid profiles clustering closely together (Fig. 1B). The pH of supernatants was also different between fructose (pH = ~ 6) and organic acids (pH = ~8.5) indicating distinct metabolic routes. Different carbon sources are known to modulate secondary metabolite production (Duffy and Défago, 1999; Ruiz et al., 2010). For example,

*Pseudomonas chlororaphis* SPB1217 produces more phenazines when grown in the presence of malate than fructose (Shtark et al., 2003). Other factors like bacterial lifestyle and temperature also influence metabolite production. Biofilm formation can lead to overproduction of phenazines and pyrrolnitrin in *P. chlororaphis* JV395B (Rieusset et al., 2020), and temperature affects *Pseudomonas* metabolite production (Tribelli and López, 2022).

However, we observed a greater impact of strain relatedness (Fig. 1A, PERMANOVA  $R^2 = 0.35$ ,  $F = 40.03$ ,  $p < 0.001$ ) compared to carbon sources on *Pseudomonas* metabolomes (Fig. 1A, PERMANOVA,  $R^2 = 0.19$ ,  $F = 21.63$ ,  $p < 0.001$ ). *P. fluorescens* JV391\_D17 and JV391\_D10, which share 86–90 % of their genes (Table 2), exhibited the most similar metabolomes, that were distinct from those of JV395B and F113 (Fig. 1C). *P. chlororaphis* JV395B, harboring 40 % of specific genes, showed a distinct metabolome from *P. ogarae* F113 (37 % specific genes) and from the two *P. fluorescens* strains. This suggests that the OGI activity in JV395B and F113 might be linked to their specific genes, as their metabolomes were consistently distinct in the PCA analyses (Fig. 1C). Previous studies confirmed that JV395B and F113 produce unique metabolites, like phloroglucinol compounds for F113 and phenazines for JV395B (Rieusset et al., 2022, 2021, 2020).

#### 4.2. Comparative metabolomic enables the identification of new OGI metabolites

In our study, the use of four strains and four carbon sources enabled the production of a wide variety of metabolites in supernatants with varying levels of OGI activity. JV391\_D17, displaying hardly any OGI activity, served as a *Pseudomonas* background allowing the exclusion of common inactive metabolites.

OGI activities in supernatants could stem from: i) specific molecules like phloroglucinol compounds (PG, MAPG, DAPG) produced by wild-type *P. ogarae* F113 (Lurthy et al., 2023), ii) over-production of OGI molecules, such as DAPG in F113 grown with pyruvate versus fructose (Table S6), or iii) synergistic effects between different molecules. Previous studies have noted synergies between *Pseudomonas* biocontrol molecules, such as phenazines and rhamnolipids, which enhance suppression of *Pythium* spp. or by the combined action of cyclopeptides with cell-wall degrading enzymes of *P. syringae* (Fogliano et al., 2002; Perneel et al., 2008).

Our results suggest that OGI activity also depends on broomrape species and their host specificity. For instance, F113 pyruvate-supernatant inhibited the germination of *P. ramosa* pv. rapeseed (86 %) more effectively than that of *P. ramosa* pv. tobacco (14 %) (Table 1). These differences can be attributed to varying sensitivities of broomrape species and pathovars to phloroglucinol compounds like PG, MAPG, and DAPG, which exhibit different lethal concentrations across broomrape species and pathovars (Lurthy et al., 2023). The same variations in OGI activity have been observed on *O. crenata*, *O. cumana*, *O. minor* and *P. ramosa* with some plant allelochemicals and several fungal phytotoxins (Cimmino et al., 2014). The metabolite profiles of *Pseudomonas*, shaped by interactions with the host plant, are likely to play a role in the biosynthesis of microbial inhibitors that may target broomrape germination in different ways. Different wheat cultivars have been shown to modulate the production of *Pseudomonas* metabolites involved in biocontrol (Rieusset et al., 2021; Valente et al., 2020), suggesting that selecting host plant cultivars that promote OGI production could be a strategy to mitigate broomrape infestation.

A global metabolomic approach was used to explore numerous ions potentially linked to OGI activity in *Pseudomonas* supernatants (Fig. 1, Fig. 2, Fig. S3 and Fig. S4), though this approach has inherent limitations. Despite their similar metabolomic profiles (Fig. 1C), *P. fluorescens* JV391\_D10 exhibited greater OGI activity than JV391\_D17 with all carbon sources. The primary ions driving separation in PCA analyses are not consistently associated with OGI activity, and the lack of comprehensive chemical databases for *Pseudomonas*-produced metabolites

complicates the identification of these ions. Thus, while global analyses are useful for identifying OGI metabolites in genetically distant *Pseudomonas* strains, they may be less effective for closely related strains. Multivariate analysis might overlook significant differences that univariate tests could reveal, as OGI activities in JV391\_D10 may involve only a limited subset of metabolites (Saccenti et al., 2014). Therefore, identifying all *Pseudomonas* metabolites displaying OGI activity from the vast diversity of potential ions remains challenging, but comparative metabolomics could facilitate the selection of a smaller subset of ions for further investigation, as we did through clustering analyses based on their accumulation patterns.

Thanks to the metabolomic analysis of a fractionated supernatant of JV395B, we identified OGI activity in a subset of polar ions, reducing potential candidates associated to OGI activity (Fig. 2B). We then correlated the accumulation of polar ions with OGI activity and identified an ion with a mass of 375 g/mol (real mass 374 g/mol in positive mode) and a retention time of 65 s. In the MetaboAnalyst database (Pang et al., 2024), this ion is annotated as isocucurbit acid glucoside. However, since this compound is not known to be produced by bacteria yet, this annotation should be verified, as online databases like MetaboAnalyst are not specialized in microbial metabolites. This ion is not unique to the JV395B strain but appears to be overproduced in supernatants from this strain, especially in the presence of fructose and pyruvate. The overproduction of M375T65 by JV391\_D10 and JV391\_D17 when using fumarate as the carbon source is consistent with the OGI activity observed for these strains under these conditions (Table 1).

Our work highlighted the limit of metabolomic analyses with the actual tools of purification, data annotation and molecule identification. Several attempts were conducted to purify the fraction containing the M375T65 ion but it co-purifies with salts and sugars from the supernatant. These highly polar compounds, more abundant than M375T65, made purification extremely difficult, despite testing multiple gradient concentrations. In the future, expanding bacterial databases in metabolomic studies should facilitate the identification of previously unknown molecules.

#### 4.3. Targeted metabolomic identified new OGI metabolites

In addition to a global metabolomic approach, we conducted a targeted analysis by identifying known specialized metabolites in *Pseudomonas* supernatants (Table 3). Not all predicted secondary metabolites identified from literature and genome-mining analyses could be annotated in the metabolite profiles of the four strains. This result was expected because the production of some metabolites requires specific substrates, such as tryptophan for producing auxin compounds like IAA (Fett et al., 1987) or pyrrolnitrin (Pawar et al., 2019) and adenine for producing cytokinin compounds like *trans*-zeatin (García de Salamone et al., 2001). In contrast, phloroglucinol compounds and phenazines were found in the supernatants of F113 and JV395B, respectively.

Among the specifically produced metabolites, phloroglucinol compounds in F113, known for their OGI activity, were correlated with the toxicity of F113 supernatants to broomrape (Table 1, Table 3, Table S6) (Lurthy et al., 2023). The siderophore dimethyl-2, 6-pyridinedicarboxylate (PDC), known to chelate various metals and thereby to inhibit their potential toxicity (Cortese et al., 2002), was also present in F113 but is not associated with any OGI activity and has a low toxicity on broomrapes. JV395B produced antifungal compounds, such as the common phenazine (PCA) and hydroxylated derivatives of PCA (OH-PHZ: hydroxyphenazine) (Rieusset et al., 2020). OH-PHZ had OGI activity on *P. ramosa* but its accumulation in supernatant was not related to the contrasted levels of JV395B's OGI activity according to the carbon source. Both PDC and phenazines have a specific ability to chelate metals in addition to the common fluorescent *Pseudomonas* pyoverdines that were shown to be produced in F113 and JV395B. In our study, we did not detect any siderophores other than pyoverdines. Even though specific pyoverdines of rhizosphere *Pseudomonas* exhibit high

antagonistic activity by competing with phytopathogens for iron (Gu et al., 2020; Robin et al., 2007), our results suggest that siderophores did not contribute to the OGI activity of the four *Pseudomonas* strains.

Regarding organic acids, malate and citrate were found more frequently present in JV391\_D17 and JV391\_D10 supernatants whereas succinate and fumarate were more frequently present in JV395B and F113 supernatants. Differences in organic acid accumulation have been observed in *Pseudomonas* strains and associated with their potential role in phosphate solubilization (Vyas and Gulati, 2009), as well as in metal chelation (Lurthy et al., 2021).

Compounds such as pyrrolnitrin, pyoluteorin, 2,4-diacetylphloroglucinol (DAPG), phenazine, and cytokinin were very effective in inhibiting broomrape germination under *in vitro* conditions, especially against *P. ramosa* pv. rapeseed (Table 3). These *Pseudomonas* compounds are well-documented for their diverse antimicrobial and phytotoxic properties, but their anti-broomrape effects are recognized for the first time in this study. The mode of action of these molecules on broomrape germination is not yet known. According to the literature on their antifungal activities, DAPG, pyrrolnitrin and pyoluteorin could disrupt the germination process of broomrape seeds by interfering with the integrity and function of cellular membranes (Kwak et al., 2011; Mishra and Arora, 2018; Pawar et al., 2019). Phenazine compounds, known for their redox-active properties, may generate reactive oxygen species that can cause oxidative stress and damages to the seeds (Biessy and Filion, 2018; Mishra and Arora, 2018). Cytokinins, a class of plant growth regulators, can disrupt the hormonal balance within broomrape seeds, inhibiting germination by interfering with the regulation of cell division and growth processes (Sosnowski et al., 2023). Collectively, these *Pseudomonas* compounds may contribute to an unfavorable microenvironment for broomrape seed germination through a combination of direct biocidal effects and indirect modulation of host plant defense mechanisms.

#### 4.4. The biocontrol activity of *Pseudomonas* on rapeseed against *P. ramosa* can be transposed to the greenhouse

All OGI metabolite-producing *Pseudomonas* strains reduced broomrape infestation by limiting parasite attachment. *P. chlororaphis* JV395B, which exhibited the best OGI activity under *in vitro* experiment (Table 1), was also the most effective as a biocontrol agent against broomrapes (Fig. 3C). Previous research demonstrated that IAA and salicylic acid (SA) could trigger plant-induced systemic resistance (ISR), protecting lentils and faba beans from *O. crenata* broomrape infestations in both pots and fields (Briache et al., 2023, 2020). Interestingly, the four *Pseudomonas* strains used in this study produced SA in their supernatants (Table 3) and harbor genes involved in Trp-dependent IAA biosynthesis pathways, an amino acid supplied in soil by plant roots (Yue et al., 2014). Moreover, the biocontrol activity against broomrapes may be enhanced by the ability of *Pseudomonas* strains to produce other ISR-inducing metabolites, such as pyoverdines (all strains), phenazines (JV395B), and DAPG (F113). These metabolites are known to protect various plants, such as rice, beans, and *Arabidopsis*, against pathogens like *Magnaporthe oryzae*, *Rhizoctonia solani*, *Peronospora parasitica*, and *Pseudomonas syringae* pv. tomato (Iavicoli et al., 2003; Ma et al., 2016; Stringlis et al., 2018; Weller et al., 2012).

#### 4.5. *Pseudomonas* strains offer a good potential in broomrape biocontrol

The production of various OGI metabolites can be optimized by i) selecting natural *Pseudomonas* strains that overexpress OGI compounds or ii) providing carbon sources like fumarate, which can induce OGI production in many *Pseudomonas* strains effective against different broomrapes (Table 1). Fumarate, costing approximately 42 €/kg, could be a valuable addition to biocontrol formulations, as it can inhibit broomrape germination ( $IC_{50} = 545 \mu\text{M}$ ) on its own. Similarly, using complex plant-derived media could promote a wide range of OGI

metabolites in *Pseudomonas* due to their diverse carbon sources (Rieusset et al., 2022).

## 5. Conclusion

This study highlights the significant potential of *Pseudomonas* strains in the biocontrol of parasitic plants, specifically broomrape species, by producing orobanche growth inhibition (OGI) metabolites. The research demonstrates that the production of these metabolites is influenced by both the carbon source used and the genetic diversity of the bacterial strains. Notably, certain *Pseudomonas* metabolites, such as phloroglucinol compounds and phenazines, exhibit strong inhibitory effects on broomrape germination, with the effectiveness varying across different species and pathovars of the parasite.

Our study showed that, in addition to the well-characterized OGI molecules, *Pseudomonas* genomes may harbor gene clusters involved in the biosynthesis of other, yet undiscovered, OGI compounds. Even though identification of M375T65, the most discriminant ion, was not achieved with the current metabolomic tools, the data on the molecule's mass and retention time is a meaningful result.

The findings suggest that optimizing the production of OGI metabolites through targeted selection of *Pseudomonas* strains and manipulation of growth conditions could enhance their biocontrol efficacy. This approach offers a promising alternative to chemical herbicides, particularly for crops like rapeseed that are vulnerable to broomrape infestations. These results also indicate the potential for extending these biocontrol strategies to other crops affected by parasitic plants, underscoring the broader applicability of *Pseudomonas*-based solutions in sustainable agriculture.

## CRedit authorship contribution statement

**Marjolaine Rey:** Methodology, Investigation. **Pierre-Edouard Mercier:** Methodology, Investigation. **Tristan Lurthy:** Writing – original draft, Methodology, Investigation, Data curation, Conceptualization. **Florence Gerin:** Investigation. **Claire Prigent-Combaret:** Writing – review & editing, Supervision, Investigation, Funding acquisition. **Gilles Comte:** Writing – review & editing. **Florence Wisniewski-Dyé:** Writing – review & editing, Investigation.

## Funding

This research and TL were supported by two grants from the French National Research Agency “Ecophyto Maturation” (ANR-19-ECOM-0002 WeedsBiocontrol) and “France Relance”.

## Conflict of interest

The authors declare no conflict of interest.

## Competing interests

None declared.

## Declaration of Competing Interest

The authors declare the following financial interests/personal relationships which may be considered as potential competing interests: Prigent-Combaret Claire reports financial support was provided by National Centre for Scientific Research. Prigent-Combaret Claire reports financial support was provided by French National Research Agency. Lurthy Tristan reports financial support was provided by French National Research Agency. If there are other authors, they declare that they have no known competing financial interests or personal relationships that could have appeared to influence the work reported in this paper.

## Acknowledgements

We thank the research team US2B of Nantes and more specifically Jean-Bernard Pouvreau for providing the broomrape seeds. We thank the company RAGT for providing seeds of the oilseed rape cultivars. We thank members of the Rhizo team of the Microbial Ecology unit at University Lyon 1 for their help in enumeration of broomrapes bound to *B. napus* roots in greenhouse. We are most grateful to the platform “Serre” of FR BioEEnViS (University Lyon 1) where plant protection assays were carried out. We also thank the Lyon Ingénierie Projet team from University Lyon 1 for its useful support.

## Appendix A. Supporting information

Supplementary data associated with this article can be found in the online version at [doi:10.1016/j.micres.2024.127933](https://doi.org/10.1016/j.micres.2024.127933).

## Data availability

Data will be made available on request.

## References

- Bally, R., Comte, G., Bernillon, J., Bellvert, F., Prigent-Combaret, C., Duponnois, R., Wisniewski-Dyé, F., Bertrand, C., Miche, L., 2017. Use of a dicarboxylic acid to control the growth of holoparasitic or hemiparasitic plants. *FR3020241B1*.
- Bennett, J.R., Mathews, S., 2006. Phylogeny of the parasitic plant family Orobanchaceae inferred from phytochrome A. *Am. J. Bot.* 93, 1039–1051. <https://doi.org/10.3732/ajb.93.7.1039>.
- Biessy, A., Filion, M., 2018. Phenazines in plant-beneficial *Pseudomonas* spp.: biosynthesis, regulation, function and genomics. *Environ. Microbiol.* 20, 3905–3917. <https://doi.org/10.1111/1462-2920.14395>.
- Brazelton, J.N., Pfeufer, E.E., Sweat, T.A., Gardener, B.B.M., Coenen, C., 2008. 2,4-Diacetylphloroglucinol alters plant root development. *MPMI* 21, 1349–1358. <https://doi.org/10.1094/MPMI-21-10-1349>.
- Briache, F.Z., Ennami, M., Mbasani-Mansi, J., Lozzi, A., Abousalim, A., Rodeny, W.E., Amri, M., Triqui, Z.E.A., Mentag, R., 2020. Effects of salicylic acid and indole acetic acid exogenous applications on induction of Faba Bean resistance against *Orobanche crenata*. *Plant Pathol.* J. 36, 476–490. <https://doi.org/10.5423/PPJ.OA.03.2020.0056>.
- Briache, F.Z., Amri, M.E., Ennami, M., Amri, M., Triqui, Z.E.A., Mentag, R., 2023. Induction of systemic resistance to *Orobanche crenata* in lentil by exogenous application of salicylic acid and indole acetic acid. *J. Plant Prot. Res.* 63, 83–96. <https://doi.org/10.24425/jppr.2023.144506>.
- Cain, C.C., Lee, D., Waldo, R.H., Henry, A.T., Casida, E.J., Wani, M.C., Wall, M.E., Oberlies, N.H., Falkingham, J.O., 2003. Synergistic antimicrobial activity of metabolites produced by a nonobligate bacterial predator. *Antimicrob. Agents Chemother.* 47, 2113–2117. <https://doi.org/10.1128/AAC.47.7.2113-2117.2003>.
- Cartry, D., Steinberg, C., Gibot-Leclerc, S., 2021. Main drivers of broomrape regulation. *A review. Agron. Sustain. Dev.* 41, 17. <https://doi.org/10.1007/s13593-021-00669-0>.
- Cimmino, A., Fernández-Aparicio, M., Andolfi, A., Basso, S., Rubiales, D., Evidente, A., 2014. Effect of fungal and plant metabolites on broomrapes (*Orobanche* and *Phelipanche* spp.) seed germination and radicle growth. *J. Agric. Food Chem.* 62, 10485–10492. <https://doi.org/10.1021/jf504609w>.
- Cortese, M.S., Paszczynski, A., Lewis, T.A., Sebat, J.L., Borek, V., Crawford, R.L., 2002. Metal chelating properties of pyridine-2,6-bis(thiocarboxylic acid) produced by *Pseudomonas* spp. and the biological activities of the formed complexes. *Biomaterials* 15, 103–120. <https://doi.org/10.1023/A:1015241925322>.
- Dadon, T., Nun, N.B., Mayer, A.M., 2004. A factor from *Azospirillum brasilense* inhibits germination and radicle growth of *Orobanche aegyptiaca*. *Isr. J. Plant Sci.* 52, 83–86. <https://doi.org/10.1560/Q3BA-8BJW-W7GH-XHPX>.
- Duffy, B.K., Défago, G., 1999. Environmental factors modulating antibiotic and siderophore biosynthesis by *Pseudomonas fluorescens* biocontrol strains. *Appl. Environ. Microbiol.* 65, 2429–2438. <https://doi.org/10.1128/AEM.65.6.2429-2438.1999>.
- Fett, W.F., Osman, S.F., Dunn, M.F., 1987. Auxin production by plant-pathogenic *Pseudomonas* and *Xanthomonas*. *Appl. Environ. Microbiol.* 53, 1839–1845. <https://doi.org/10.1128/aem.53.8.1839-1845.1987>.
- Fogliano, V., Ballio, A., Gallo, M., Woo, S., Scala, F., Lorito, M., 2002. *Pseudomonas* lipodepsipeptides and fungal cell wall-degrading enzymes act synergistically in biological control. *MPMI* 15, 323–333. <https://doi.org/10.1094/MPMI.2002.15.4.323>.
- García de Salamone, I.E., Hynes, R.K., Nelson, L.M., 2001. Cytokinin production by plant growth promoting rhizobacteria and selected mutants. *Can. J. Microbiol.* 47, 404–411. <https://doi.org/10.1139/w01-029>.
- Gealy, D.R., Gurusiddaiah, S., Ogg, A.G., 1996. Isolation and characterization of metabolites from *Pseudomonas syringae* -strain 3366 and their phytotoxicity against certain weed and crop species. *Weed Sci.* 44, 383–392. <https://doi.org/10.1017/S0043174500094042>.
- Giacomoni, F., Le Corguillé, G., Monsoor, M., Landi, M., Pericard, P., Pétera, M., Duperier, C., Tremblay-Franco, M., Martin, J.-F., Jacob, D., Goullitquier, S., Thévenot, E.A., Caron, C., 2015. Workflow4Metabolomics: a collaborative research infrastructure for computational metabolomics. *Bioinformatics* 31, 1493–1495. <https://doi.org/10.1093/bioinformatics/btu813>.
- Gibot-Leclerc, S., Guinchard, L., Edel-Hermann, V., Dessaint, F., Cartry, D., Reibel, C., Gautheron, N., Bernaud, E., Steinberg, C., 2022. Screening for potential mycoherbicides within the endophyte community of *Phelipanche ramosa* parasitising tobacco. *FEMS Microbiol. Ecol.* 642, 1–12. <https://doi.org/10.1093/femsec/fiac024>.
- Gu, S., Wei, Z., Shao, Z., Friman, V.-P., Cao, K., Yang, T., Kramer, J., Wang, X., Li, M., Mei, X., Xu, Y., Shen, Q., Kümmerli, R., Jousset, A., 2020. Competition for iron drives phytopathogen control by natural rhizosphere microbiomes. *Nat. Microbiol.* 5, 1002–1010. <https://doi.org/10.1038/s41564-020-0719-8>.
- Hallett, S.G., 2005. Where are the bioherbicides? *Weed Sci.* 53, 404–415. <https://doi.org/10.1614/WS-04-157R2>.
- Hasannejad, S., Zad, S.J., Alizade, H.M., Rahymian, H., 2006. The effects of *Fusarium oxysporum* on broomrape (*Orobanche aegyptiaca*) seed germination. *Commun. Agric. Appl. Biol. Sci.* 71, 1295–1299.
- Huet, S., Pouvreau, J.-B., Delage, E., Delgrange, S., Marais, C., Bahut, M., Delavault, P., Simier, P., Poulin, L., 2020. Populations of the parasitic plant *Phelipanche ramosa* influence their seed microbiota. *Front. Plant Sci.* 11, 1075. <https://doi.org/10.3389/fpls.2020.01075>.
- Iavicoli, A., Boutet, E., Buchala, A., Métraux, J.-P., 2003. Induced systemic resistance in *Arabidopsis thaliana* in response to root inoculation with *Pseudomonas fluorescens* CHA0. *Mol. Plant Microbe Interact.* 16, 851–858. <https://doi.org/10.1094/MPMI.2003.16.10.851>.
- Joel, D.M., 2009. The new nomenclature of *Orobanche* and *Phelipanche*. *Weed Res.* 49, 6–7. <https://doi.org/10.1111/j.1365-3180.2009.00748.x>.
- Kawa, D., Thiombiano, B., Shimels, M., Taylor, T., Walmsley, A., Vahldick, H.E., Leite, M. F., Musa, Z., Bucksch, A., Dini-Andreote, F., Chen, A.J., Daksa, J., Etalo, D., Tessema, T., Kuramae, E.E., Raaijmakers, J.M., Bouwmeester, H., Brady, S.M., 2022. The soil microbiome reduces *Striga* infection of sorghum by modulation of host-derived signaling molecules and root development. *bioRxiv*. (<https://doi.org/10.1101/2022.11.06.515382>).
- Keel, C., 1992. Suppression of root diseases by *Pseudomonas fluorescens* CHA0: importance of the bacterial secondary metabolite 2,4-diacetylphloroglucinol. *MPMI* 5, 4. <https://doi.org/10.1094/MPMI-5-004>.
- Kremer, R.J., Souissi, T., 2001. Cyanide production by rhizobacteria and potential for suppression of weed seedling growth. *Curr. Microbiol.* 43, 182–186. <https://doi.org/10.1007/s002840010284>.
- Kwak, Y.-S., Han, S., Thomashow, L.S., Rice, J.T., Paulitz, T.C., Kim, D., Weller, D.M., 2011. *Saccharomyces cerevisiae* genome-wide mutant screen for sensitivity to 2,4-diacetylphloroglucinol, an antibiotic produced by *Pseudomonas fluorescens*. *Appl. Environ. Microbiol.* 77, 1770–1776. <https://doi.org/10.1128/AEM.02151-10>.
- Lawrance, S., Varghese, S., Varghese, E.M., Asok, A.K., S, J.M., 2019. Quinolone derivatives producing *Pseudomonas aeruginosa* H6 as an efficient bioherbicide for weed management. *Biotecol. Agric. Biotechnol.* 18, 101096. <https://doi.org/10.1016/j.bcab.2019.101096>.
- Lee, J.H., Anderson, A.J., Kim, Y.C., 2022. Root-associated bacteria are biocontrol agents for multiple plant pests. *Microorganisms* 10, 1053. <https://doi.org/10.3390/microorganisms10051053>.
- Li, A., Sun, X., Liu, L., 2022. Action of salicylic acid on plant growth. *Front. Plant Sci.* 13. <https://doi.org/10.3389/fpls.2022.878076>.
- Loper, J.E., Hassan, K.A., Mavrodi, D.V., Davis, E.W., Lim, C.K., Shaffer, B.T., Elbourne, L.D.H., Stockwell, V.O., Hartney, S.L., Breakwell, K., Henkels, M.D., Tetu, S.G., Rangel, L.L., Kidarsa, T.A., Wilson, N.L., van de Mortel, J.E., Song, C., Blumhagen, R., Radune, D., Hostetler, J.B., Brinkac, L.M., Durkin, A.S., Kluepfel, D. A., Wechter, W.P., Anderson, A.J., Kim, Y.C., Pierson, L.S., Pierson, E.A., Lindow, S. E., Kobayashi, D.Y., Raaijmakers, J.M., Weller, D.M., Thomashow, L.S., Allen, A.E., Paulsen, I.T., 2012. Comparative genomics of plant-associated *Pseudomonas* spp.: insights into diversity and inheritance of traits involved in multitrophic interactions. *PLoS Genet.* 8, e1002784. <https://doi.org/10.1371/journal.pgen.1002784>.
- Lurthy, T., Cantat, C., Jeudy, C., Declercq, P., Gallardo, K., Barraud, C., Leroy, F., Ourry, A., Lemanceau, P., Salon, C., Mazurier, S., 2020. Impact of bacterial siderophores on iron status and ionome in pea. *Front. Plant Sci.* 11, 730. <https://doi.org/10.3389/fpls.2020.00730>.
- Lurthy, T., Pivato, B., Lemanceau, P., Mazurier, S., 2021. Importance of the rhizosphere microbiota in iron biofortification of plants. *Front. Plant Sci.* 12, 744445. <https://doi.org/10.3389/fpls.2021.744445>.
- Lurthy, T., Perot, S., Gerin-Eveillard, F., Rey, M., Wisniewski-Dyé, F., Vacheron, J., Prigent-Combaret, C., 2023. Inhibition of broomrape germination by 2,4-diacetylphloroglucinol produced by environmental *Pseudomonas*. *Microb. Biotechnol.* <https://doi.org/10.1111/1751-7915.14336>.
- Ma, Z., Hua, G.K.H., Ongena, M., Höfte, M., 2016. Role of phenazines and cyclic lipopeptides produced by *Pseudomonas* sp. CMR12a in induced systemic resistance on rice and bean. *Environ. Microbiol. Rep.* 8, 896–904. <https://doi.org/10.1111/1758-2229.12454>.
- Martinez, L., Pouvreau, J.-B., Montiel, G., Jestin, C., Delavault, P., Simier, P., Poulin, L., 2023. Soil microbiota promotes early developmental stages of *Phelipanche ramosa* L. Pomel during plant parasitism on *Brassica napus* L. *Plant Soil* 483, 667–691. <https://doi.org/10.1007/s1104-022-05822-6>.

- Masteling, R., Lombard, L., de Boer, W., Raaijmakers, J.M., Dini-Andreote, F., 2019. Harnessing the microbiome to control plant parasitic weeds. *Curr. Opin. Microbiol.* 49, 26–33. <https://doi.org/10.1016/j.mib.2019.09.006>.
- Maurhofer, M., Keel, C., Haas, D., Défago, G., 1995. Influence of plant species on disease suppression by *Pseudomonas fluorescens* strain CHAO with enhanced antibiotic production. *Plant Pathol.* 44, 40–50. <https://doi.org/10.1111/j.1365-3059.1995.tb02714.x>.
- Mishra, J., Arora, N.K., 2018. Secondary metabolites of fluorescent pseudomonads in biocontrol of phytopathogens for sustainable agriculture. *Appl. Soil Ecol.* 125, 35–45. <https://doi.org/10.1016/j.apsoil.2017.12.004>.
- Müller, T., Behrendt, U., 2021. Exploiting the biocontrol potential of plant-associated pseudomonads – a step towards pesticide-free agriculture? *Biol. Control* 155, 104538. <https://doi.org/10.1016/j.biocontrol.2021.104538>.
- Mustafa, A., Naveed, M., Saeed, Q., Ashraf, M.N., Hussain, A., Abbas, T., Kamran, M., Nan-Sun, Minggang, X., 2019. Application potentials of plant growth promoting rhizobacteria and fungi as an alternative to conventional weed control methods. *Sustainable Crop Production. IntechOpen*. <https://doi.org/10.5772/intechopen.86339>.
- Mutuku, J.M., Cui, S., Yoshida, S., Shirasu, K., 2021. Orobanchaceae parasite–host interactions. *New Phytol.* 230, 46–59. <https://doi.org/10.1111/nph.17083>.
- Pang, Z., Lu, Y., Zhou, G., Hui, F., Xu, L., Viati, C., Spigelman, A.F., MacDonald, P.E., Wishart, D.S., Li, S., Xia, J., 2024. MetaboAnalyst 6.0: towards a unified platform for metabolomics data processing, analysis and interpretation. *Nucleic Acids Res.* 52, W398–W406. <https://doi.org/10.1093/nar/gkac253>.
- Parker, C., 2012. Parasitic weeds: a world challenge. *Weed Sci.* 60, 269–276. <https://doi.org/10.1614/WS-D-11-00068.1>.
- Pawar, S., Chaudhari, A., Prabha, R., Shukla, R., Singh, D.P., 2019. Microbial pyrrolnitrin: natural metabolite with immense practical utility. *Biomolecules* 9, E443. <https://doi.org/10.3390/biom9090443>.
- Perneel, M., D'hondt, L., De Maeyer, K., Adiobo, A., Rabaey, K., Höfte, M., 2008. Phenazines and biosurfactants interact in the biological control of soil-borne diseases caused by *Pythium* spp. *Environ. Microbiol.* 10, 778–788. <https://doi.org/10.1111/j.1462-2920.2007.01501.x>.
- Rieusset, L., Rey, M., Muller, D., Vacheron, J., Gerin, F., Dubost, A., Comte, G., Prigent-Combaret, C., 2020. Secondary metabolites from plant-associated *Pseudomonas* are overproduced in biofilm. *Microb. Biotechnol.* 13, 1562–1580. <https://doi.org/10.1111/1751-7915.13598>.
- Rieusset, L., Rey, M., Gerin, F., Wisniewski-Dyé, F., Prigent-Combaret, C., Comte, G., 2021. A cross-metabolomic approach shows that wheat interferes with fluorescent *Pseudomonas* physiology through its root metabolites. *Metabolites* 11, 84. <https://doi.org/10.3390/metabo11020084>.
- Rieusset, L., Rey, M., Wisniewski-Dyé, F., Prigent-Combaret, C., Comte, G., 2022. Wheat metabolite interferences on fluorescent *Pseudomonas* physiology modify wheat metabolome through an ecological feedback. *Metabolites* 12, 236. <https://doi.org/10.3390/metabo12030236>.
- Robin, A., Mazurier, S., Mougel, C., Vansuyt, G., Corberand, T., Meyer, J.-M., Lemanceau, P., 2007. Diversity of root-associated fluorescent pseudomonads as affected by ferritin overexpression in tobacco: diversity of fluorescent pseudomonads in rhizosphere. *Environ. Microbiol.* 9, 1724–1737. <https://doi.org/10.1111/j.1462-2920.2007.01290.x>.
- Rubiales, D., Alcántara, C., Pérez-de-Luque, A., Gil, J., Sillero, J., 2003. Infection of chickpea (*Cicer arietinum*) by cretate broomrape (*Orobanche crenata*) as influenced by sowing date and weather conditions. *Agronomy* 23, 359–362. <https://doi.org/10.1051/agro:2003016>.
- Ruiz, B., Chávez, A., Forero, A., García-Huante, Y., Romero, A., Sánchez, M., Rocha, D., Sánchez, B., Rodríguez-Sanoja, R., Sánchez, S., Langley, E., 2010. Production of microbial secondary metabolites: Regulation by the carbon source. *Crit. Rev. Microbiol.* 36, 146–167. <https://doi.org/10.3109/10408410903489576>.
- Saccetti, E., Hoefsloot, H.C.J., Smilde, A.K., Westerhuis, J.A., Hendriks, M.M.W.B., 2014. Reflections on univariate and multivariate analysis of metabolomics data. *Metabolomics* 10, 361–374. <https://doi.org/10.1007/s11306-013-0598-6>.
- Shahid, I., Malik, K.A., Mehnaz, S., 2018. A decade of understanding secondary metabolism in *Pseudomonas* spp. for sustainable agriculture and pharmaceutical applications. *Environ. Sustain.* 1, 3–17. <https://doi.org/10.1007/s42398-018-0006-2>.
- Shanahan, P., O'sullivan, D.J., Simpson, P., Glennon, J.D., O'gara, F., 1992. Isolation of 2,4-diacetylphloroglucinol from a fluorescent pseudomonad and investigation of physiological parameters influencing its production. *Appl. Environ. Microbiol.* 58, 353–358.
- Shirley, M., Avoscan, L., Bernaud, E., Vansuyt, G., Lemanceau, P., 2011. Comparison of iron acquisition from Fe–pyoverdine by strategy I and strategy II plants. *Botany* 89, 731–735. <https://doi.org/10.1139/b11-054>.
- Shtark, O.Yu., Shaposhnikov, A.I., Kravchenko, L.V., 2003. The Production of antifungal metabolites by *Pseudomonas chlororaphis* grown on different nutrient sources. *Microbiology* 72, 574–578. <https://doi.org/10.1023/A:1026047301457>.
- Sosnowski, J., Truba, M., Vasileva, V., 2023. The impact of auxin and cytokinin on the growth and development of selected crops. *Agriculture* 13, 724. <https://doi.org/10.3390/agriculture13030724>.
- Spaepen, S., Bossuyt, S., Engelen, K., Marchal, K., Vanderleyden, J., 2014. Phenotypical and molecular responses of *Arabidopsis thaliana* roots as a result of inoculation with the auxin-producing bacterium *Azospirillum brasilense*. *New Phytol.* 201, 850–861. <https://doi.org/10.1111/nph.12590>.
- Stringlis, I.A., Yu, K., Feussner, K., de Jonge, R., Van Bentum, S., Van Verk, M.C., Berendsen, R.L., Bakker, P.A.H.M., Feussner, I., Pieterse, C.M.J., 2018. MYB72-dependent coumarin exudation shapes root microbiome assembly to promote plant health. *PNAS* 115, E5213–E5222. <https://doi.org/10.1073/pnas.1722335115>.
- Tribelli, P.M., López, N.I., 2022. Insights into the temperature responses of *Pseudomonas* species in beneficial and pathogenic host interactions. *Appl. Microbiol. Biotechnol.* 106, 7699–7709. <https://doi.org/10.1007/s00253-022-12243-z>.
- Vacheron, J., Moëgne-Loccoz, Y., Dubost, A., Gonçalves-Martins, M., Muller, D., Prigent-Combaret, C., 2016. Fluorescent *Pseudomonas* strains with only few plant-beneficial properties are favored in the maize rhizosphere. *Front. Plant Sci.* 7. <https://doi.org/10.3389/fpls.2016.01212>.
- Valente, J., Gerin, F., Le Gouis, J., Moëgne-Loccoz, Y., Prigent-Combaret, C., 2020. Ancient wheat varieties have a higher ability to interact with plant growth-promoting rhizobacteria. *Plant Cell Environ.* 43, 246–260. <https://doi.org/10.1111/pce.13652>.
- Vandenkoornhuise, P., Quaiser, A., Duhamel, M., Le Van, A., Dufresne, A., 2015. The importance of the microbiome of the plant holobiont. *New Phytol.* 206, 1196–1206. <https://doi.org/10.1111/nph.13312>.
- Vyas, P., Gulati, A., 2009. Organic acid production *in vitro* and plant growth promotion in maize under controlled environment by phosphate-solubilizing fluorescent *Pseudomonas*. *BMC Microbiol.* 9, 174. <https://doi.org/10.1186/1471-2180-9-174>.
- Weller, D.M., Mavrodi, D.V., van Pelt, J.A., Pieterse, C.M.J., van Loon, L.C., Bakker, P.A.H.M., 2012. Induced systemic resistance in *Arabidopsis thaliana* against *Pseudomonas syringae* pv. tomato by 2,4-diacetylphloroglucinol-producing *Pseudomonas fluorescens*. *Phytopathology* 102, 403–412. <https://doi.org/10.1094/PHYTO-08-11-0222>.
- Yue, J., Hu, X., Huang, J., 2014. Origin of plant auxin biosynthesis. *Trends Plant Sci.* 19, 764–770. <https://doi.org/10.1016/j.tplants.2014.07.004>.